Impact behaviour of triggered and non-triggered crash tubes with auxetic lattices

Usta, F., Ertaş, O. F., Ataalp, A., Türkmen, H. S., Kazancı, Z., & Scarpa, F. (2019). Impact behaviour of triggered and non-triggered crash tubes with auxetic lattices. *Multiscale and Multidisciplinary Modeling, Experiments and Design*, *2*(2), 119-127. https://doi.org/10.1007/s41939-018-00040-z

Published in:
Multiscale and Multidisciplinary Modeling, Experiments and Design

Document Version:
Peer reviewed version

IMPACT BEHAVIOUR OF TRIGGERED AND NON-TRIGGERED CRASH TUBES WITH AUXETIC LATTICES

Fatih Usta[1], Osman F. Ertaş[1], Altuğ Ataalp[1], Halit S. Türkmen[1], Zafer Kazancı[2], Fabrizio Scarpa[3]

[1]Faculty of Aeronautics and Astronautics, Istanbul Technical University, Maslak, Istanbul, 34469, Turkey

[2]Advanced Composites Research Group, School of Mechanical and Aerospace Engineering, Queen's University Belfast, Belfast BT9 5AH, United Kingdom

[3]Bristol Composites Institute (ACCIS), University of Bristol, Bristol BS8 ITR, United Kingdom

Fatih Usta: ustaf@itu.edu.tr

Osman F. Ertas: ertastos@itu.edu.tr

Altuğ Ataalp: ataalpaltug@gmail.com

Halit S. Türkmen: halit@itu.edu.tr

Zafer Kazancı: Z.Kazanci@qub.ac.uk

Fabrizio Scarpa: F.Scarpa@bristol.ac.uk

Keywords: Crash tube, Auxetic materials, Impact loading, Energy absorption.

ABSTRACT

In this study, impact behavior of triggered and non-triggered tubes with and without auxetic filler are examined by using numerical methods. Material properties of tubes made of aluminum alloy and auxetic lattices utilizing ABSplus plastics are determined by using tensile tests. Finite element analyses are performed by using LS-DYNA software at 5 m/s impact velocity. Two different trigger shape are suggested and compared each other and discussed the advantages and disadvantages over non-triggered tubes. For these loading conditions, trigger mechanism provides lower peak forces and higher crash force efficiency (CFE), but lower specific energy absorption (SEA). Also, the effects of using auxetic fillers in these triggered tubes are investigated in terms crashworthiness characteristics.

1. INTRODUCTION

Thin walled tubes convert part of the kinetic energy during collision to plastic energy, and therefore help to prevent the crash and damage. Besides, inertial loads, which occur at the beginning of the collision, can be also quite harmful for passengers during a dynamic crash. Metallic cylindrical tubes are widely used as structural components of automobiles (Abdollahpoor and Marzbanrad (2010)).

In the literature, there are several studies on the impact behavior of crash box. The main objective of these studies is to increase the crashworthiness of crash boxes. For this purpose, geometrical modifications on tubes, various cross section types and material types have been examined to obtain better designs. For example, Usta et al. (2015, 2017 and 2018) studied on stepped and concentric circular crash tubes under axial impact loading by using numerical, experimental and optimization techniques. Eyvazian et al. (2014) investigated the effects of corrugations on the deformation behavior, energy absorption, and failure mode of circular aluminum tube and show that corrugated tubes provided higher crashworthiness characteristics. Lee et al. (1999) analyzed metallic tubes including grooves at folding sites where could be pre-estimated by FEA analysis. Triggering improved the energy absorption performance and half-dented tube were more effective than full-dented tube. On the contrary, energy absorption could be worsen by using triggering without consideration of the peak location of the folding wave and inhomogeneous deformation. The geometry of the trigger mechanism could be optimized by using various methods (Marsolek and Reimerdes (2004)). Hage et al. (2005) investigated various types of trigger mechanism of metallic tubes such as chamfering, triangular hole pattern and geometric imperfection. Force displacement response and folding mechanism could be controlled by changing trigger types.

As folding material, foams and conventional honeycombs are generally used in the tube structures. Beside the traditional honeycombs and foams, auxetic lattices have been studied in recent years. Auxetic lattices are preferable, because anisotropic material properties increase the impact and indentation resistance and energy and shock absorption absorption performance. A prior study on auxetic materials belongs to Lakes (1987) in the literature. Auxetic materials have different usage area such as crash helmets, body armour, sports clothing. For example, Yang et al. (2018) analyzed the auxetic performance of a conventional and two auxetic honeycomb structure subjected to dynamic and static loading. They provided that using auxetic structures in the sandwich structures have higher shock absorption over non-auxetic structure.

Density and modulus of auxetic structures can be controlled during fabrication which provides to be obtained auxetic structure as required in terms of Poisson ratio (Duncan et. al (2018)). Hou et al. (2018) compared a uniform cell design with a present functionally gradient auxetic celluler structure subjected to low speed collision. Impact tests demonstrated that gradient auxetic crash box has higher energy absorption and lower reaction force than uniform auxetic crash box. In another study, Jiang and Hu (2017) tested PU foam, auxetic and non auxetic composite structures under low velocity impact and showed that auxetic composite have better energy absorption performance in medium strain range. Direnberger et. al. (2013) proved the advantages of the auxetic materials in comparison with honeycombs. Yang et al. (2011) indicated that re-entrant honeycomb structure had good ability of energy absorption under compression load. Lim at al. (2014) investigated the auxetic behavior of polyurethane foam under impact loading. According to their work, auxetic foams could have no advantages over conventional foams under high velocity impact.

For a conventional material, the dog bone specimen elongates in axial direction while its cross section area is shrinking. Therefore, the sign of Poisson's ratio becomes positive. On the other hand, the sign of the Poisson's ratio of the auxetic materials is negative. Some researchers examined the mechanical properties of auxetic tubular structures under compression and tension loads (Ren et al. (2016)) and resistance to kinking (Karnessis and Burriesci (2013)).

In this work, circular crash tubes with and without auxetic lattices are examined under dynamic loads from a numerical perspective. The novel designs of trigger mechanism on crash tubes are introduced and discussed the shape and location of the triggering with consideration of the re-entrant lattices. Two different trigger mechanism are applied to the tube system and compared with the conventional one. The effects of using triggering on tube structures are investigated. Besides, this paper focuses on the exploration the possibility of using auxetic materials with the combination of trigger mechanism in crashworthiness performance of metallic tubes. Impact behavior of re-entrant honeycomb filled tubes are compared with empty tubes.

2. DETERMINING MATERIAL PROPERTIES

2.1 Material properties of AL6063 aluminum alloy

The tubes considered here is made of aluminum alloy AA6063. Owing to insensitivity of aluminum on strain rate, tensile tests are carried out under quasi static loading at 2 mm/min velocity (Ali et al. (2015)). Six test specimens are cut by using CNC machine according to ASTM E8/E8M test standard (see, Fig. 1). Biaxial strain gauges are stuck and extensometers are located to define material properties. Material properties of each sample are determined and listed in Table 1. Random errors are estimated according to average value of Young modulus, yield stress and ultimate tensile strength which are 67.69 GPa, 160 MPa, and 192 MPa, respectively. Poisson ratio and density are 0.3 and 2710 kg/m^3. No significant differences are observed between the stress and strain curves of tested specimens. Engineering stress and strain curve is plotted in Fig 2.

Figure 1: Tensile test specimens of AL6063 aluminum alloy.

Table 1: Mechanical properties and random errors of AL6063 aluminum alloy.

Specimen No	Young Modulus (GPa)	Random Error %	Yield Stress (MPa)	Error %	Ultimate Tensile Stress (MPa)	Random Error %
1	70.44	4.06	145	9.47	182	5.29
2	65.33	3.49	165	3.02	195	1.47
3	65.49	3.25	151	5.72	180	6.33
4	66.12	2.32	172	7.39	202	5.12
5	71.27	5.29	173	8.01	210	9.28
6	67.49	0.30	155	3.23	184	4.25
Average	67.69		160		192	

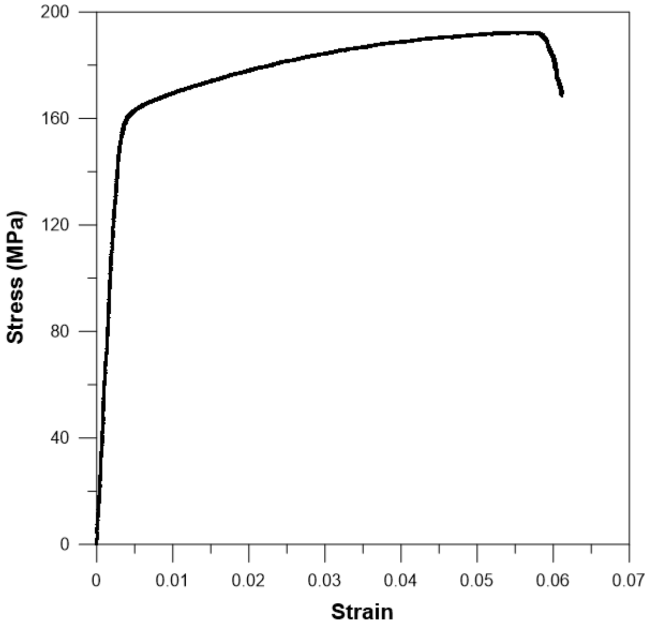

Figure 2: Engineering stress and strain curve of AL6063 tube.

2.2 Material properties of ABSplus plastics

The auxetic lattice is made of ABSplus plastics. Strain rate has significant effects on mechanical properties of ABS plus plastics (Rodríguez (2001)). In this study, tensile tests of ABSplus plastic are revealed under quasi static loading due to having no possibility of SHPB test system. Four test specimens are produced with FDM (fused deposition modeling) technology by using Dimension Elite 3D printer machine (see, Fig. 3). Specimens are printed at roam temperature (effective temperature range 15-30 ^{0}C) and interior filling style is selected as solid which provides more durable and stronger parts. After performing tension tests, mechanical properties of each sample and random errors are determined (see, Table 2). Average Young modulus is 1.53 GPa, ultimate tensile strength is 23.25 MPa, yield stress is 19.73 MPa, density is 1040 kg/m^3 and Poisson's ratio is 0.36. Engineering stress and strain curve is plotted in Fig. 4.

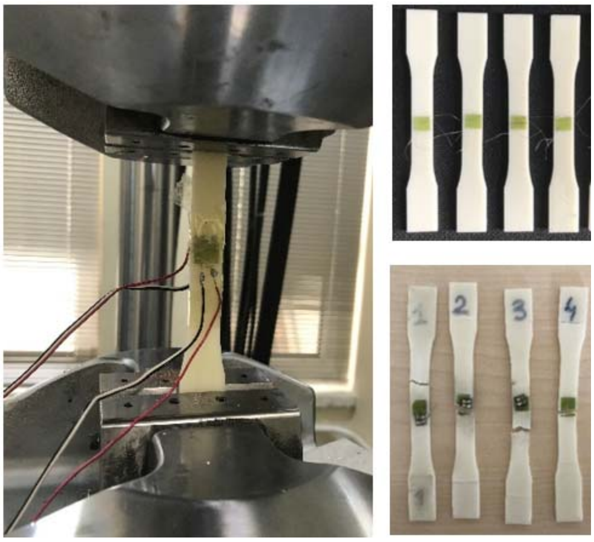

Figure 3: Tensile test specimens of ABSplus plastics.

Table 2: Mechanical properties and random errors of ABSplus plastics.

Specimen No	Young Modulus (GPa)	Random Error %	Yield Stress (MPa)	Error %	Ultimate Tensile Stress (MPa)	Random Error %
1	1.58	3.10	16.8	14.83	21.8	6.24
2	1.39	9.30	21.5	9.00	24.1	3.66
3	1.48	3.43	18.2	7.73	22.8	1.94
4	1.68	9.62	22.4	13.56	24.3	4.52
Average	1.53		19.73		23.25	

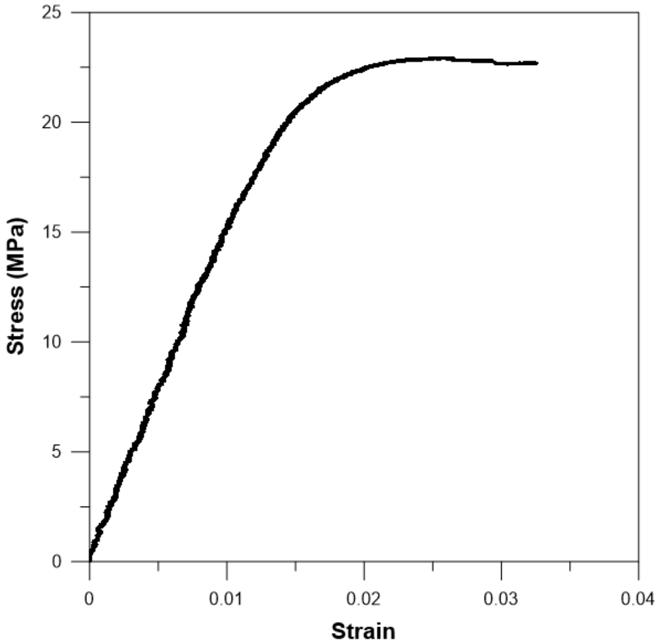

Figure 4: Engineering stress and strain curve of ABSplus plastics.

3. TUBE DESIGNS AND FINITE ELEMENT MODELING

3.1. Finite Element Modeling

The numerical studies are conducted by using LS-DYNA software, which is based on explicit time integration method and desirable program especially for dynamic crash analysis. A rigid mass is dropped on the tubes with a speed of 5 m/s. Rigidwall_Planar_Moving_Forces is used as an impactor to model the impact behavior. The nodes at the bottom of the tube structure are clamped. A schematic view of tube and rigid impactor is plotted in Figure 5. Three different tube structures with and without re-entrant honeycomb structure are investigated. The diameter, length and thickness of the tubes are 70, 100 and 2 mm, respectively. Auxetic filler type is chosen as re-entrant honeycomb owing to its wider capacity of negative Poisson ratio range in comparison with the other auxetic geometries (Elipe and Lantada (2012)). Scarpa et al. (2000) show that geometric cell parameters of reentrant honeycomb have significant effects on the mechanical properties such as in plane Poisson ratio and young modulus. The cell parameters of re-entrant honeycomb θ, h, l and t are 30^0, 10 mm, 10 mm and 1 mm.

Tubes and auxetic fillers are modeled by using Belytschko-Tsay shell elements. This element formulation gives greater computational efficiency compared with other shell element formulations (Hallquist, 2006). Optimum element size is defined as 2 mm x 2 mm, after comparing the results of analysis of crash tubes at different mesh qualities. Automatic single surface contact algorithms are identified for each specimen, because they have possibility of lapping after deformation. Also, automatic surface to surface contact interface is defined between surfaces of tube and auxetic filler. The static and dynamic friction coefficients are chosen as 0.2 and 0.3 respectively for each contact definition.

The Material model of aluminum tube and plastic auxetic lattice are defined with MAT24 (Piecewise Linear Plasticity) material card in LS-DYNA. Elastic material properties of tube and auxetic lattice are used in this material card. True stress and effective plastic strain curve is embedded into this material card for the plasticity of these material. Effective plastic strain is derived from the difference of true strain and the ratio of true stress over Young modulus.

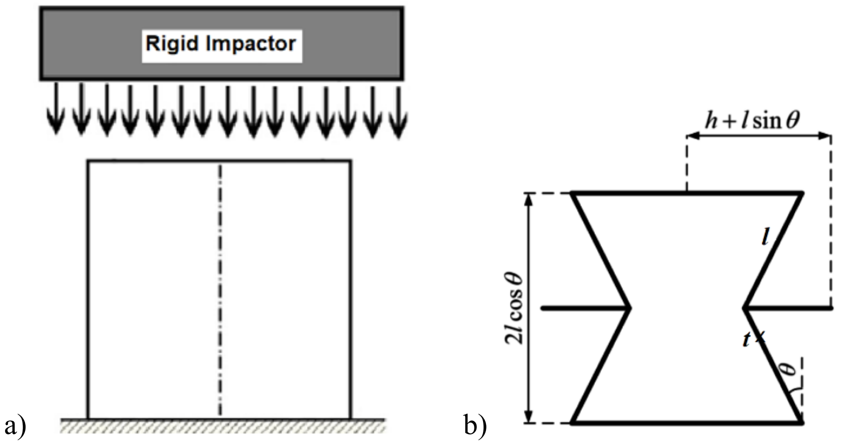

Figure 5: a) Schematic view of rigid impactor and tube, b) re-entrant honeycomb cell parameters.

3.2. Tube Designs

The first model does not have any triggering on the tube structure so that it is abbreviated as NT (non-triggered) as shown in Fig. 6. Empty tube is abbreviated as "E" and auxetic filler is abbreviated as "A". The number in the name of model denotes tube length in terms of millimeter.

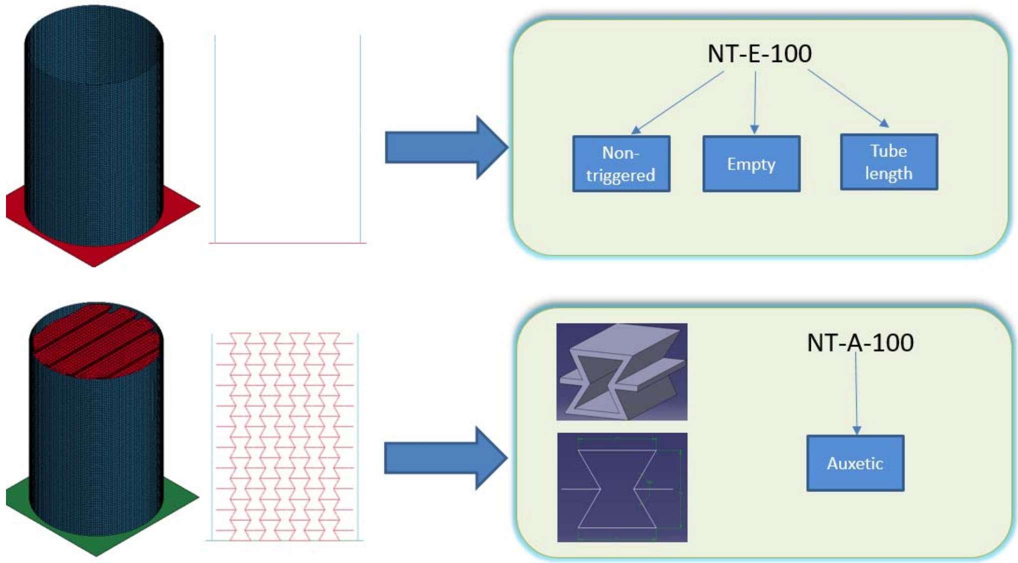

Figure 6: NT-E and NT-A models.

Second and third model include imperfection on the tubes. Trigger mechanism of second model is an arc, as shown in Fig. 7. Due to circular shape, it is named as circular trigger (CT). Trigger shape of the third model is like in zigzag geometry, as shown in Fig. 8. Because it consists of lines, it is named as Line Triggered (LT). It is aimed to control the crash stability and collapse modes and to increase crashworthiness characteristics of tubes by using these trigger shapes. The distance between two arc and two zigzag lines are chosen as 10 mm and the corner points of them are in same level.

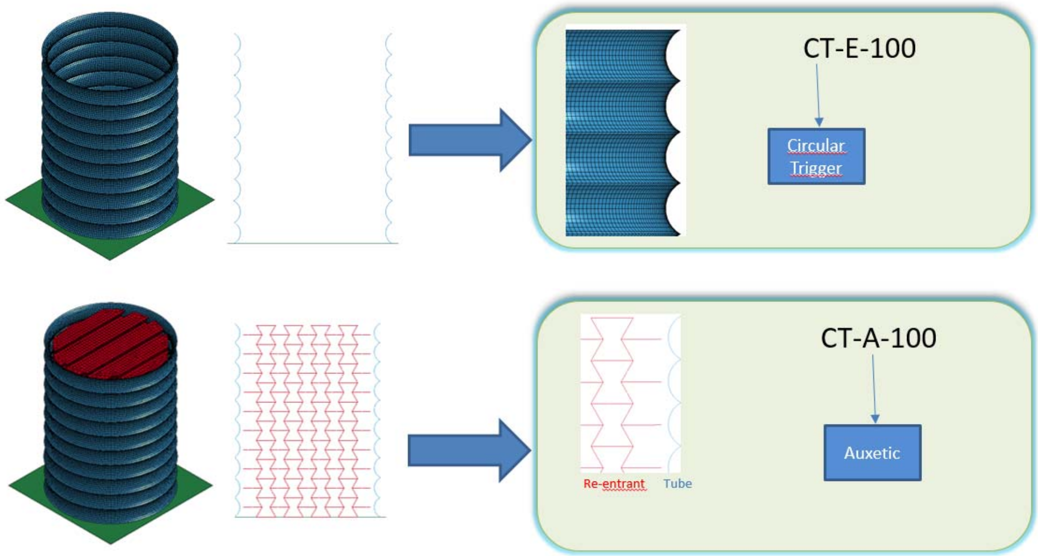

Figure 7: CT-E and CT-A models.

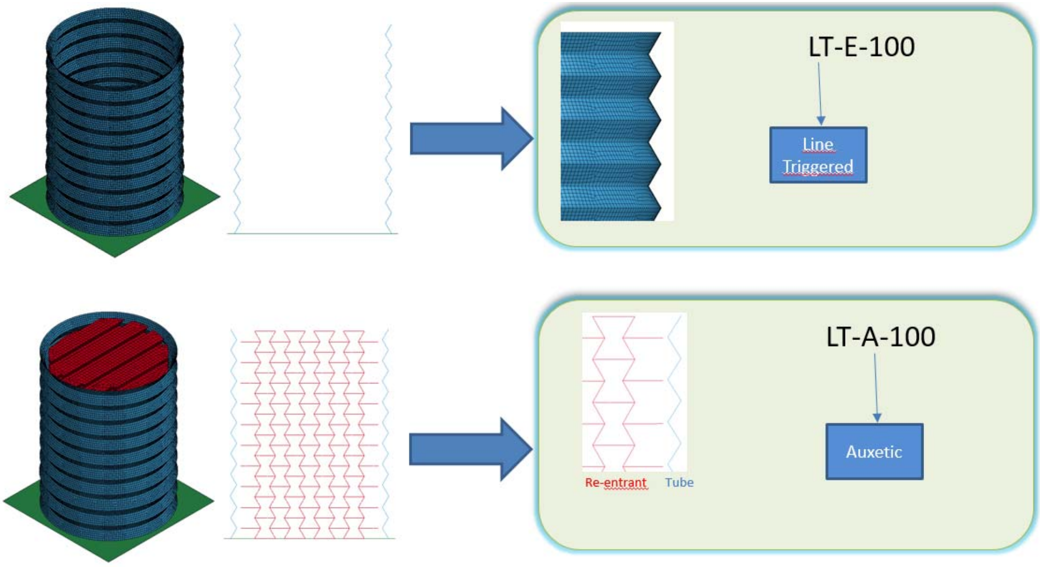

Figure 8: LT-E and LT-A models.

4. RESULTS AND DISCUSSION

4.1. Formulation of Parameters Used for Comparisons

For the comparison study, some crashworthiness characteristics are used listed as below. Energy Absorption (EA), PCF (Peak Crash Force) Specific Energy Absorption (SEA), Mean Crushing Force (MCF) and Crash Force Efficiency (CFE) are the most common parameters to represent the crash behavior. Energy absorption of the tube under crash load can be expressed as:

$$EA = \int_0^{\delta} P(s)ds \tag{1}$$

where δ is the axial deformation of the structure and P(s) denotes the axial crash force. SEA is calculated as absorbed energy divided by mass:

$$SEA = \frac{EA}{m} \tag{2}$$

Peak crash force means maximum force value in the axial direction:

$$PCF = \max(P(s)) \tag{3}$$

MCF is calculated as absorbed energy divided by the amount of deformation:

$$MCF = \frac{\mathrm{EA}}{\delta} = \frac{\int_0^{\delta} P(s)ds}{\delta} \tag{4}$$

Crash force efficiency is calculated as MCF divided by PCF.

$$CFE = \frac{P_m}{PCF} \tag{5}$$

4.2. The effects of length of the tubes on crashworthiness characteristics

To investigate the effects of the tubes on crashworthiness characteristics, all models are analyzed by changing tube length with the length of 100, 125 and 150 mm. The results are compared in terms of reaction force response in time and collapse mechanism. The results show that shorter tubes are better in terms of SEA and MCF, as shown in Table 3. Tube length has no remarkable effects on the crash force response as shown in Fig. 9. Deformation of re-entrant honeycomb of NT-A-100 becomes to shrink initially at the bottom side. But for the longest non-triggered model, collapse mechanism appears at bottom and top surfaces together. Shorter tubes give better SEA and MCF values for CT and LT models. In comparison with CT and LT models with re-entrant structure, all tubes begin to collapse from top surfaces as shown in Figs. 10 and 11. In contrast to Non-triggered model, first buckling of CT and LT tubes reveal in the middle section. Therefore, it can be said that trigger system can affect the deformation behavior of filler.

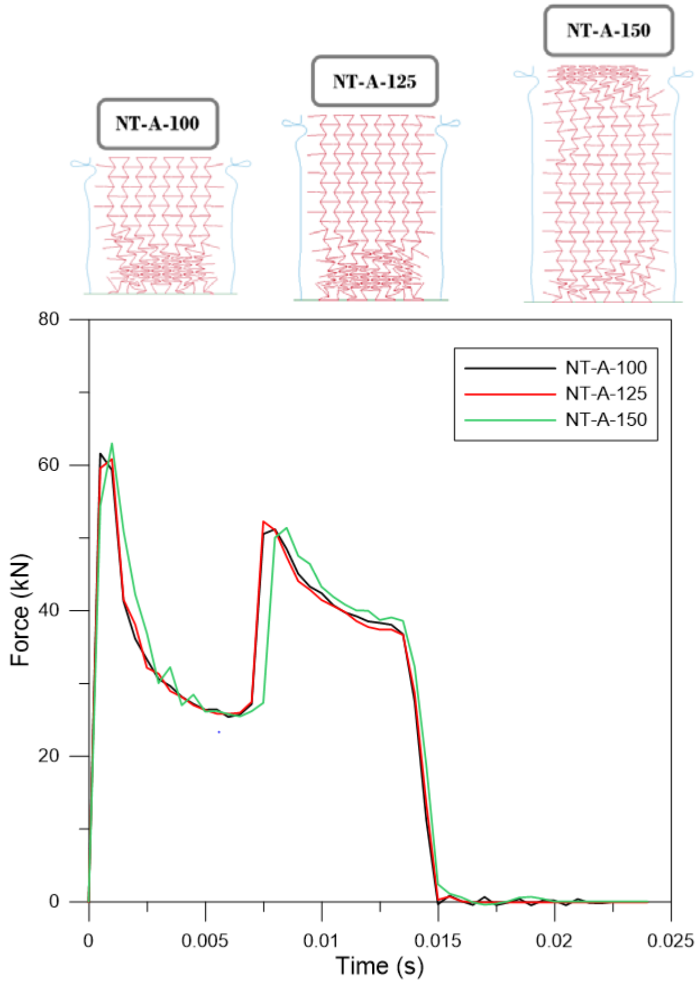

Figure 9: Comparison of deformation and force response of NT-A models.

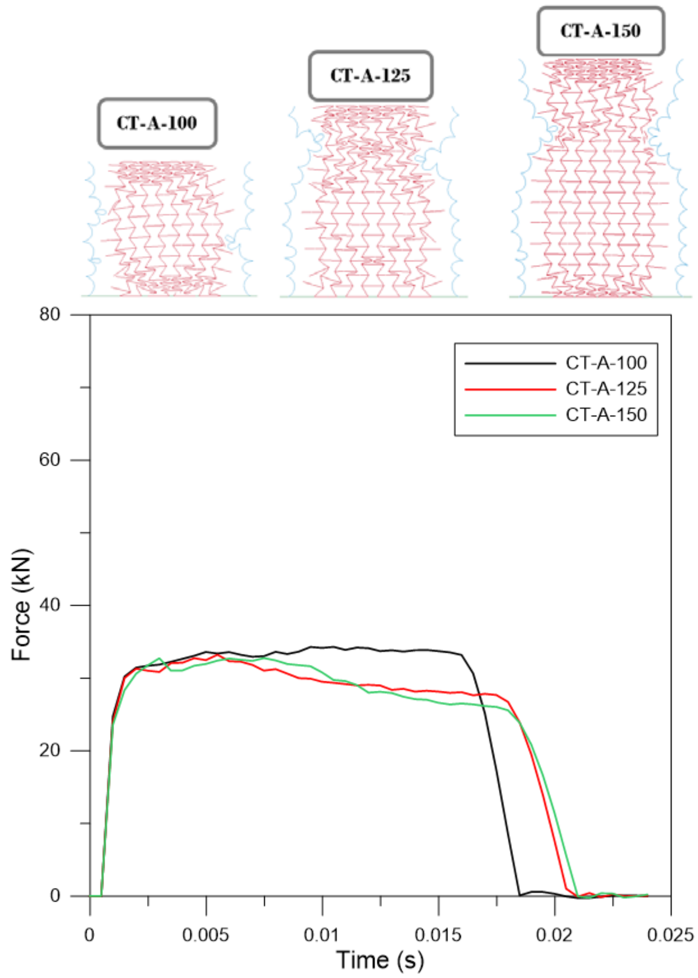

Figure 10: Comparison of deformation and force response of CT-A models.

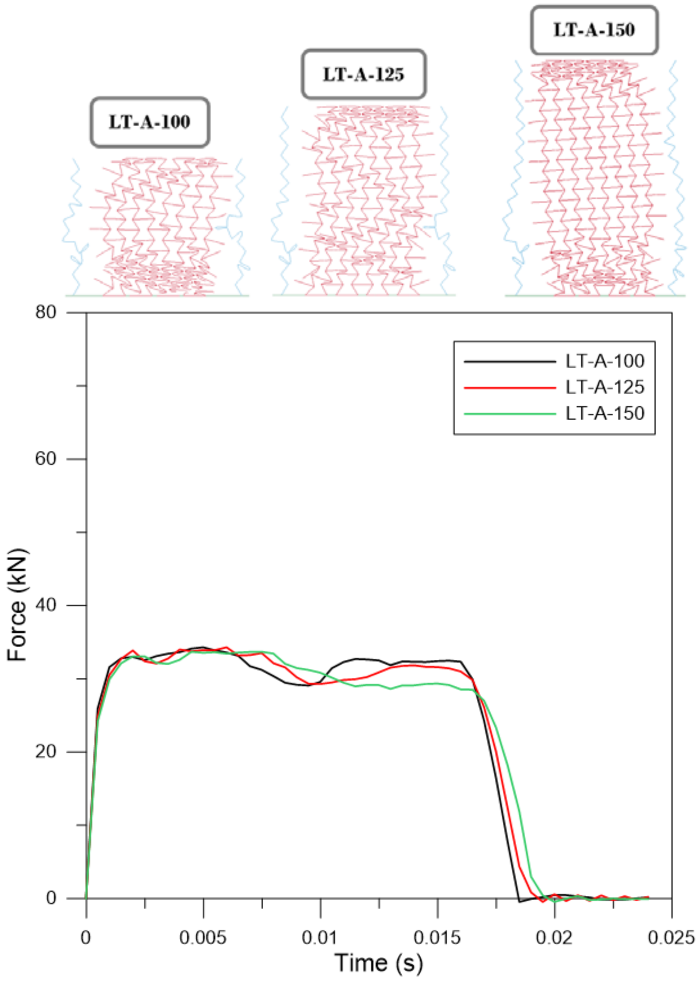

Figure 11: Comparison of deformation and force response of LT-A models.

4.2. Comparison between triggered and non-triggered tube designs

Another comparison study is performed between impact behavior of the triggered and non-triggered tubes with auxetic lattice. Crash force response of NT-A-100, CT-A-100 and LT-A-100 models are plotted in Fig 12. There is a remarkable difference between force response of non-triggered and triggered tubes. Initial peak crash forces are almost 62 kN and 34 kN, respectively. Although two different peak forces are observed for non-triggered tubes, initial and subsequent force values of triggered tubes become similar. It can be strictly effective on the inertial effects of crash loads on passenger. It is achieved a great reduction of this inertial loads owing to small difference between subsequent forces of triggered tubes.

In Table 3, results show that Non triggered tubes have advantages over triggered tubes in terms of MCF and SEA due to higher durability under buckling and bending loads and lower mass. On the other hand, in terms of peak force and crash force efficiency triggered tubes are obviously better than non-triggered tubes. CFE is the final decisive parameter to determine the most efficient tube design due to including three important results in one formulation. The triggering changes the deformation mode and increases the energy absorption capacity of the axially compressed tubes.

In comparison with the results of triggered tubes, and peak crash force change of CT tubes is smoother than LT tubes. Therefore it is more useful in terms of inertial loads. But CT tubes are deflected more than LT tubes in axial direction and also its arc geometry cause to more mass. Therefore LT tubes are better than CT tubes in terms of MCF and CFE. Table 3 illustrates that LT-A-100/125/150 are superior to other types of tubes in terms of CFE.

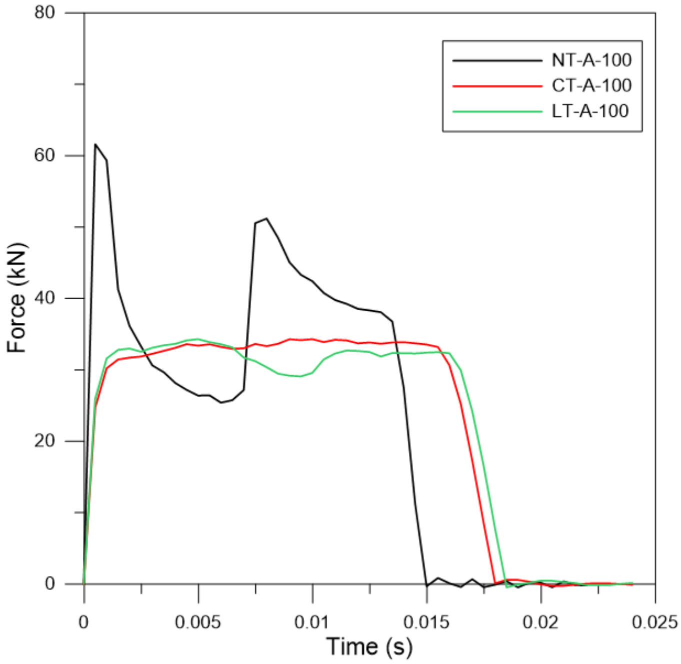

Figure 12: Comparison of force response of different samples with auxetic filler.

Table 3: Crashworthiness parameters of tubes with auxetic filler.

Models	**PCF (kN)**	**Deflection (mm)**	**Mass (kg)**	**SEA (kJ/kg)**	**MCF (kN)**	**CFE**
NT-A-100	61.62	32.70	0.2258	5.491	37.912	0.615
CT-A-100	34.35	39.78	0.2560	4.838	31.141	0.907
LT-A-100	34.28	39.32	0.2512	4.934	31.524	0.920
NT-A-125	60.89	32.74	0.2817	4.396	37.827	0.621
CT-A-125	33.22	41.13	0.3180	3.911	30.235	0.910
LT-A-125	34.29	39.46	0.3132	3.967	31.483	0.918
NT-A-150	62.97	33.55	0.3375	3.676	36.983	0.587
CT-A-150	32.75	41.22	0.3821	3.242	30.049	0.917
LT-A-150	33.73	39.73	0.3750	3.313	31.265	0.927

4.3. The effects of using auxetic lattices on crashworthiness characteristics

In Table 4, the last comparison study is seen between empty and filled tubes. It is seen that using re-entrant honeycomb has small effects on the PCF values, axial deformation and efficiency. For example, PCF values of Non-triggered empty and auxetic filled tubes are 60.8 and 61.62 kN, crash force efficiency values are 0.614 and 0.615, respectively. Contrary to a conventional honeycomb, the cross section area of the re-entrant honeycomb reduces under compression loads due to its negative Poisson's ratio. Therefore, the contact surfaces can be reduced and contact forces between the aluminum tube and auxetic material are lower than between the tube and a traditional honeycomb folding. This contact tends to reduce the peak forces on the specimen. Besides, auxetic lattices tend to increase the stiffness of the tube structure during the compressive load phase and can absorb totally more energy than empty tubes. However, re-entrant honeycomb structure can be easily deform and have a smaller effect on the deflection and brings scarcely any improvement in terms of MCF. This improvement cannot visibly overcome the decline in CFE due to higher peak forces. Accordingly, CFE values of tubes with and without auxetic filler are close each other.

In addition, it brings two times higher mass than empty tubes which leads to lower SEA values and there is a notable decline in energy absorption capability.

Table 4: Crashworthiness parameters of tubes with and without auxetic filler.

Models	**PCF (kN)**	**Deflection (mm)**	**Mass (kg)**	**SEA (kJ/kg)**	**MCF (kN)**	**CFE**
NT-E-100	60.80	33.43	0.1187	10.513	37.333	0.614
NT-A-100	61.62	32.70	0.2258	5.491	37.912	0.615
CT-E-100	33.01	40.62	0.1490	8.366	30.686	0.929
CT-A-100	34.35	39.78	0.2560	4.838	31.141	0.907
LT-E-100	33.62	40.25	0.1442	8.664	31.038	0.923
LT-A-100	34.28	39.32	0.2512	4.934	31.524	0.920

5. CONCLUSION

In this study, triggered and non-triggered tubes with and without auxetic honeycomb structure are analyzed by using LS-DYNA software under dynamic impact loading. The ability of two different trigger system according to non-triggered tubes is investigated and the effects of using arc and line shape on triggered tubes are evaluated. Triggered tubes with auxetic honeycomb have not been studied before. This paper also focus on advantages and disadvantages of using auxetic honeycomb structure in the triggered tubes under crash load. The effects of trigger mechanism, auxetic lattice and length of specimen are compared in terms of PCF, SEA, MCF and CFE values. The results are listed as below:

- Shorter tubes can provide higher SEA, MCF.
- Triggered tubes are obviously better in terms of peak crash force and crash force efficiency.

Trigger system affects the deformation behavior of re-entrant structure. Peak crash force change of CT tubes is smoother than LT tubes. Therefore it is more useful in terms of inertial loads. On the other hand, LT tubes are better than CT tubes in terms of MCF and CFE due to lower deformation in axial direction.

- CFE values of tubes with and without auxetic filler are close each other. Re-entrant honeycomb brings two times higher mass of specimen so that SEA values of specimens with auxetic lattices are lower than empty tubes.
- Table 3 illustrates LT-A-100/125/150 are superior to other types of tubes with auxetic filler in terms of CFE which is our decisive parameters to choose the better design. This result indicates the Line triggering is the best choice according to our study. Desirable models can be obtained by changing triggering shape of tube design and geometry of auxetic structures.

Acknowledgment

Support for this work has been provided by the Scientific and Technological Research Council of Turkey under Project Number 115M465.

REFERENCES

Abdollahpoor, A., & Marzbanrad, J. (2010). Crashworthiness study of axial impact in cylindrical aluminium tubes. Journal of Mechanical Engineering-Strojnícky časopis, 61, 1.

Ali, M., Ohioma, E., Kraft, F., & Alam, K. (2015). Theoretical, numerical, and experimental study of dynamic axial crushing of thin walled pentagon and cross-shape tubes. Thin-Walled Structures, 94, 253-272.

Dirrenberger, J., Forest, S., & Jeulin, D. (2013). Effective elastic properties of auxetic microstructures: anisotropy and structural applications. International Journal of Mechanics and Materials in Design, 9(1), 21-33.

Duncan, O., Allen, T., Foster, L., Gatt, R., Grima, J. N., & Alderson, A. (2018). Controlling density and modulus in auxetic foam fabrications—-implications for impact and indentation testing. MDPI Proceedings, 2(6), 250.

El-Hage, H., Mallick, P. K., & Zamani, N. (2005). A numerical study on the quasi-static axial crush characteristics of square aluminum tubes with chamfering and other triggering mechanisms. International Journal of Crashworthiness, 10(2), 183-196.

Elipe, J. C. Á., & Lantada, A. D. (2012). Comparative study of auxetic geometries by means of computer-aided design and engineering. Smart Materials and Structures, 21(10), 105004.

Eyvazian, A., Habibi, M. K., Hamouda, A. M., & Hedayati, R. (2014). Axial crushing behavior and energy absorption efficiency of corrugated tubes. Materials & Design (1980-2015), 54, 1028-1038.

Hallquist, J.O. (2006). LS-DYNA Theory Manual Livermore Software Technology Corporation 3: 25-31.

Hou, W., Yang, X., Zhang, W., & Xia, Y. (2018). Design of energy-dissipating structure with functionally graded auxetic cellular material. International Journal of Crashworthiness, 23(4), 366-376.

Jiang, L., & Hu, H. (2017). Low-velocity impact response of multilayer orthogonal structural composite with auxetic effect. Composite Structures, 169, 62-68.

Karnessis, N., & Burriesci, G. (2013). Uniaxial and buckling mechanical response of auxetic cellular tubes. Smart Materials and Structures, 22(8), 084008.

Lakes, R. S. (1987). U.S. Patent No. 4,668,557. Washington, DC: U.S. Patent and Trademark Office.

Lee, S., Hahn, C., Rhee, M., & Oh, J. E. (1999). Effect of triggering on the energy absorption capacity of axially compressed aluminum tubes. Materials & design, 20(1), 31-40.

Lim, T. C., Alderson, A., & Alderson, K. L. (2014). Experimental studies on the impact properties of auxetic materials. physica status solidi (b), 251(2), 307-313.

Marsolek, J., & Reimerdes, H. G. (2004). Energy absorption of metallic cylindrical shells with induced non-axisymmetric folding patterns. International Journal of Impact Engineering, 30(8-9), 1209-1223.

Ren, X., Shen, J., Ghaedizadeh, A., Tian, H., & Xie, Y. M. (2016). A simple auxetic tubular structure with tuneable mechanical properties. Smart Materials and Structures, 25(6), 065012.

Rodríguez, J. F., Thomas, J. P., & Renaud, J. E. (2001). Mechanical behavior of acrylonitrile butadiene styrene (ABS) fused deposition materials. Experimental investigation. Rapid Prototyping Journal, 7(3), 148-158.

Scarpa, F., Panayiotou, P., & Tomlinson, G. (2000). Numerical and experimental uniaxial loading on in-plane auxetic honeycombs. The Journal of Strain Analysis for Engineering Design, 35(5), 383-388.

Usta, F., Eren, Z., Turkmen, H. S., Kazancı, Z., Mecitoglu, Z. (2015). Numerical investigation of stepped concentric crash tubes subjected to axial impact: The effects of number of tubes, Recent Advances in Space Technologies (RAST), 2015 7th International Conference on. IEEE, 39-43.

Usta, F., Turkmen, H. S. (2017). Crash behavior of nested tube structures with various cross sections, In Recent Advances in Space Technologies (RAST), 8th International Conference on IEEE, 23-27).

Usta, F., Eren, Z., Kurtaran, H., Türkmen, H. S., Kazancı, Z., & Mecitoglu, Z. (2018). Crashworthiness Optimization of Nested and Concentric Circular Tubes Using Response Surface Methodology and Genetic Algorithm. Latin American Journal of Solids and Structures, 15(5).

Yang, C., Vora, H. D., & Chang, Y. (2018). Behavior of auxetic structures under compression and impact forces. Smart Materials and Structures, 27(2), 025012.

Yang, S., Qi, C., Guo, D. M., & Wang, D. (2012). Energy absorption of an re-entrant honeycombs with negative Poisson's ratio. In Applied Mechanics and Materials (Vol. 148, pp. 992-995). Trans Tech Publications.